applied sciences

MDPI

Article

Dual-Band Frequency Selective Surface-Backed Reflectarray for High-Speed Ka-Band Satellites

Ahmet Hulusi Gülseren [1], Aytaç Alparslan [2] and Nurhan Türker Tokan [3,*]

[1] Department of Electrical and Electronics Engineering, Aydın Adnan Menderes University, Aydın 09010, Türkiye; agulseren@adu.edu.tr
[2] Department of Electrical and Electronics Engineering, Trakya University, Edirne 22030, Türkiye; aytac@ieee.org
[3] Department of Electronics and Communication Engineering, Yildiz Technical University, Istanbul 34220, Türkiye
* Correspondence: nturker@yildiz.edu.tr

Abstract: A dual-band, dual-polarized frequency selective surface (FSS)-backed multilayer reflectarray antenna is designed for 5G high-speed satellites operating at Ka-band uplink and downlink frequencies (20/30 GHz). A reflectarray antenna system consists of two reflectarrays that are separated from each other by an FSS layer that behaves as a planar bandpass filter at Ka-band satellite uplink frequencies. Each reflectarray antenna is designed with dual-polarized unit cells. In order to achieve a uniform phase distribution across the reflectarray surface, physical dimensions and positions of the unit cells with a fixed periodicity are carefully chosen. The FSS conductor is etched to the bottom layer of the 30 GHz reflectarray substrate to save cost and weight. The reflectarray performance is analyzed by using CST Microwave Studio and array theory. A prototype is fabricated, and the results are experimentally verified. The gain of the reflectarray is measured as 21.13 dBi and 26.94 dBi at 20 and 30 GHz, respectively. A crosspol level of more than 35 dB is observed at both frequencies. The simulated and measured results show that the proposed reflectarray is suitable for high-speed Ka-band satellites.

Keywords: 5G high speed satellite; dual band; FSS; Ka-band; multilayer; reflectarray antenna

Citation: Gülseren, A.H.; Alparslan, A.; Türker Tokan, N. Dual-Band Frequency Selective Surface-Backed Reflectarray for High-Speed Ka-Band Satellites. *Appl. Sci.* **2024**, *14*, 2928. https://doi.org/10.3390/app14072928

Academic Editors: Paulo M. Mendes, Carlos Lima and Hugo Daniel da Costa Dinis

Received: 2 March 2024
Revised: 23 March 2024
Accepted: 27 March 2024
Published: 30 March 2024

1. Introduction

To sustain the demands of 5G communication in terms of mobility and coverage, satellites and space technologies play a critical role [1]. To provide high-speed internet coverage even in remote and underserved regions and achieve unique advantages of seamless, high throughput, uninterrupted global connectivity, satellites serve as a backbone for 5G networks [2]. Progress in the satellite and launch technology pave the way for these demands, which would not be possible technically and economically with terrestrial communication that severely relies on buried fiber optic cables.

Ka-band satellite is a proven technology that provides high-speed services with higher data rates by using smaller receiving antennas [3,4]. Since antennas play a critical role in satellite communications systems, high-gain antennas are essential to operate at the receive and transmit frequencies of the Ka-band (20/30 GHz) simultaneously. Reflector antennas with high gain have served as the mainstream technology until the last decade. However, progressively increasing demands of the end users have triggered the advancement of innovative antennas in both spaceborne and user terminals. As the new generation of high-gain antennas, reflectarrays that consist of planar arrays of conductive elements are developed as an alternative to curved, bulky reflector systems [5]. Besides their superior physical properties, reflectarrays combine the advantages of phased arrays and reflectors. With the individually controllable phases of reflectarray elements, the beam of the reflectarray can be generated according to the predefined benchmarks. Although printed

reflectarrays have narrower bands compared to reflectors, they offer a practical solution for multi band antennas [6,7]. Multiband characteristic of a reflectarray can be achieved by using broadband elements [8–11], multilayer unit elements [12,13], interleaved array grids [14,15], or stacked arrays [16].

The method to be applied mostly depends on the separation of the bands and specifications on the physical structure [17]. Both multi band operation and dual linear polarization may be achieved with a single layer reflectarray [18]. However, altering the phase of the unit elements for different bands results in reduced efficiency and bandwidth performance due to the mutual coupling generated by the phasing elements of the bands on a single aperture [19]. In recent years, efforts on realization of dual-band and/or dual-orthogonal polarization has led to the usage of FSSs in reflectarrays [17,19–26]. The FSS behaves as a ground plane and reflects the signal at one of the operation bands, whereas the signal is transmitted to the bottom reflectarray at the other band of operation.

In this work, an FSS is used to isolate the reflectarrays designed to operate at the downlink and uplink frequency of the Ka-band satellite systems. With the usage of a simple ring resonator that is designed to operate as a planar bandpass filter at the downlink frequency of the Ka-band satellites, the beam is directed towards predetermined direction at two distinct frequencies. Improved gain and aperture efficiency is obtained by suppressing the mutual coupling generated due to the elements of the two reflectarrays. Instead of using a separate printed circuit board for the FSS, the conductive pattern of the single-sided FSS has been etched to the bottom side of the upper reflector, which was designed to operate at 30 GHz. The phases of the two unit cells, designed for 20 and 30 GHz reflectarrays, are calculated to radiate 20º by considering the existence of the FSSs in each case. A double-ridged horn antenna that has been oriented to the center of the reflectarrays is used as the feed antenna. The full-wave analysis of the reflectarray is evaluated numerically by CST Microwave Studio [27]. A prototype is fabricated and the performance of the reflectarray designed for transmit/receive operation is experimentally verified.

2. Proposed Unit Cell Configurations

The majority of the Ka-band high-throughput satellites (HTS) operate typically in the frequency range of 27.5–31 GHz for the uplink, whereas the 17.7–21.2 GHz band is used as the downlink. In this work, 20 GHz and 30 GHz are chosen as the design frequencies of the reflectarray with dual-band operation. The periodicity of the unit cells is determined using Equation (1) to avoid grating lobes and to obtain the required phase range [28].

$$D < \lambda/(1 + sin\ \theta) \quad (1)$$

where λ is the wavelength at the operation frequency and θ is the angle of the radiated beam. The periodicity of the unit cells for 20 and 30 GHz should be chosen equal. Thus, D of the unit cells is chosen as 6 mm, which renders orientation of the main beam direction up to $\theta = 42^{\circ}$.

Proposed unit cells for the 20 GHz and 30 GHz reflectarray are shown in Figure 1. The star shape of the 30 GHz unit cell given in Figure 1a is constructed by the combination of a square with width a and its 45° rotated version. Rogers 5870 substrate material with a thickness of $t_1 = 0.79$ mm and $\varepsilon_r = 2.33$ is chosen as the substrate material. The conductor of the FSS is etched to the reverse side of the Rogers 5870 printed circuit board. Thus, to create the pattern of the FSS and 30 GHz unit cells, two sides of the same substrate material are used. The unit cell proposed for the 20 GHz reflectarray is given in Figure 1b. It is designed as a derivative of the first iteration of the Minkowski fractal. It is composed of four circles with a diameter of half square width added to the four corners of the square. Rogers 3003 substrate ($\varepsilon_r = 3$) with $t_2 = 0.76$ mm thickness is chosen as the substrate material of the unit cell.

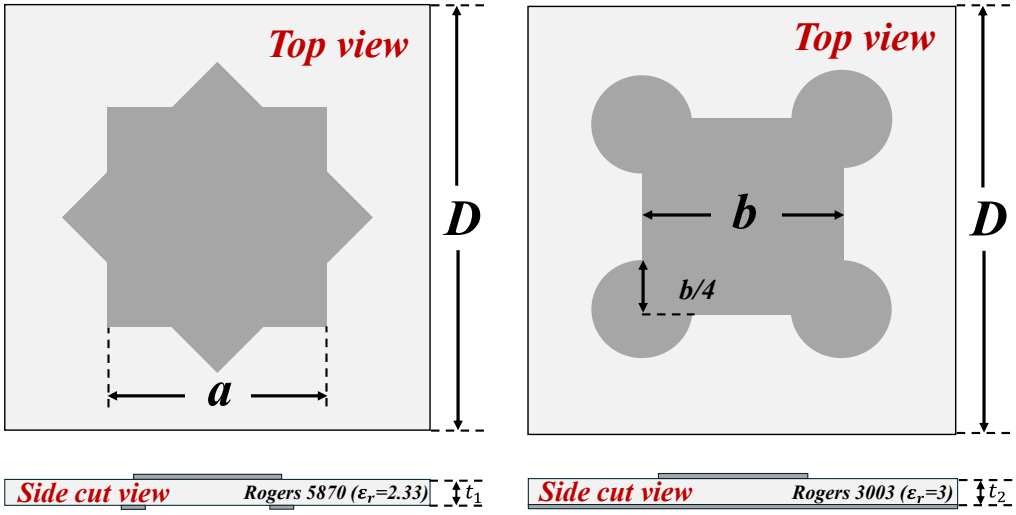

Figure 1. Proposed unit cells of the reflectarrays: (**a**) 30 GHz; (**b**) 20 GHz.

A ring-shaped conductor is used in the unit cell structure of the FSS. The FSS structure consists of a ring with $w = 0.25$ mm width and $r = 2.02$ mm radius. A 1 mm-thick air layer between the two printed circuit boards serves as the substrate of the FSS. The FSS unit cell is designed to pass wave propagation at 20 GHz and stop the 30 GHz band. S-parameters of the FSS unit cell are shown in Figure 2. The top view of the FSS is given as an inset in figure. The scattering parameters show that the FSS unit cell works as a bandpass filter up to 24 GHz and shows bandstop filter characteristics afterwards (-3 dB cutoff is considered). The dual-band reflectarray with FSS should be constructed by placing the higher frequency reflectarray to the top and lower frequency reflectarray to the bottom [29]. The FSS surface is positioned between two substrates. In our case, the reflective surface for 30 GHz will be at the top layer, while the reflective surface for 20 GHz will be at the bottom layer. The FSS structure between them will behave like a ground plane at 30 GHz and as a passband filter at 20 GHz.

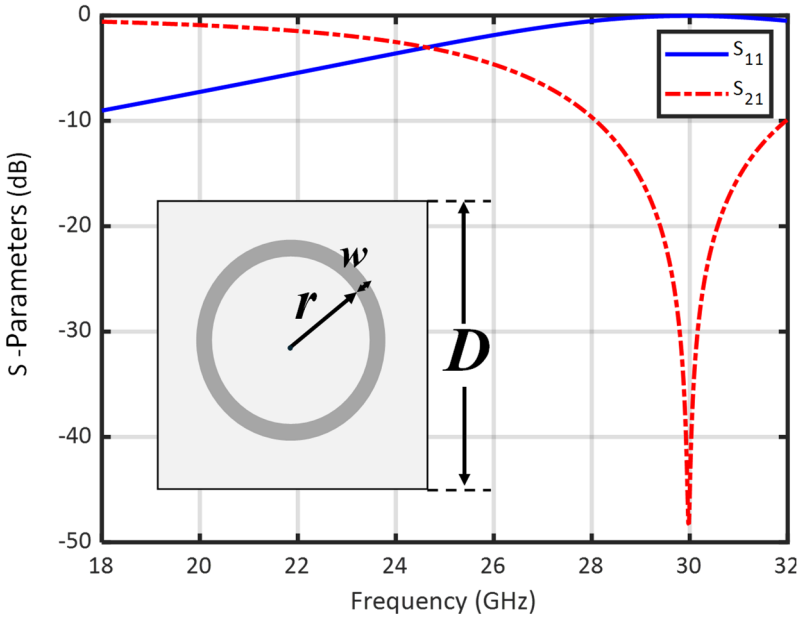

Figure 2. Scattering parameters of the FSS unit cell.

The distribution of the phases of the unit cells on the reflective surface determines the characteristic of the radiated beam. Thus, it is critical to obtain the required phase values accurately for reflectarray design. In order to obtain the phase range, a and b parameters of the unit cells are varied at the corresponding frequencies. Since FSS acts as the ground plane for the 30 GHz reflectarray, it is also included in the unit cell simulations. Similarly, FSS with air substrate and 30 GHz reflectarray unit cell are included to the unit cell simulations of the 20 GHz reflectarray. The phase variation in the multilayer structure is given in Figure 3 as the function of a parameter. An approximately 290° phase range is obtained at 30 GHz by the star shaped unit cell. This range reduces to 220° when the FSS unit cell is included. Although the FSS unit cell reduces the phase range, it should be included to the design since it enhances the reflectarray antenna performance by reducing the mutual coupling effect and providing isolation between frequency bands. The phase analysis of the 20 GHz unit cell is performed by including the FSS and 30 GHz reflectarray unit cell. As shown in Figure 3, 330° phase range is obtained at 20 GHz by varying the b parameter in the single reflectarray unit cell. It reduces to 260° when the analysis is performed with the multilayer unit cell consisting of FSS as well. This range reduces to 220° when the 30 GHz reflectarray unit cell is included. Corresponding phases of the proposed unit cells are obtained for a very small periodicity value ($D = 6$ mm). Although the inclusion of the FSS reduces the phase range of the unit cells, they are still at acceptable levels.

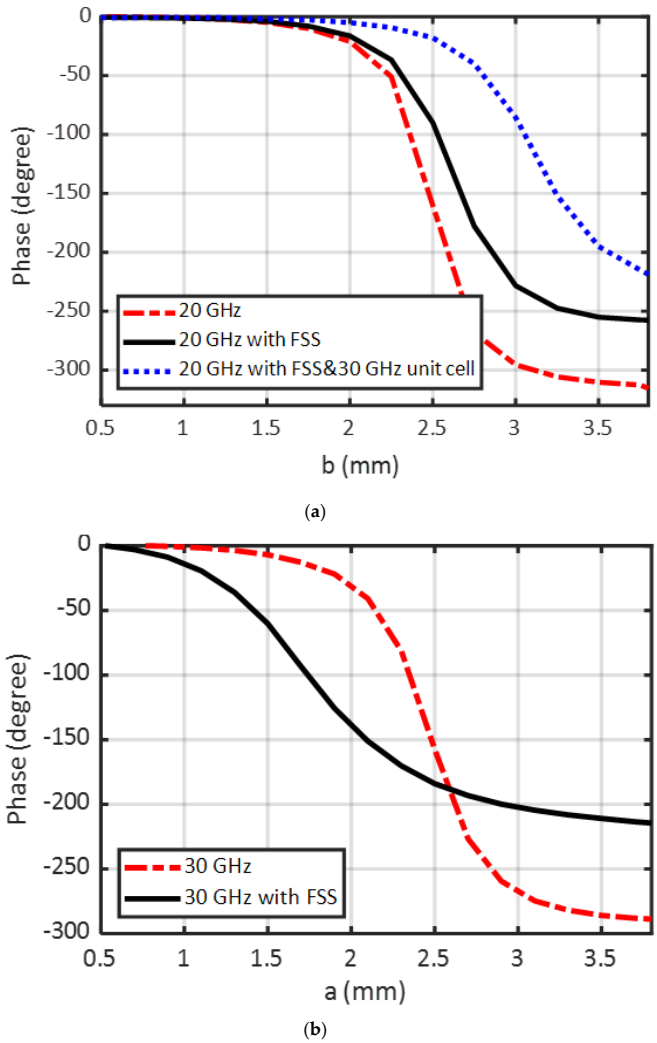

Figure 3. Phase variations of the unit cells proposed as the function of a and b parameters: (**a**) 20 GHz; (**b**) 30 GHz.

3. Dual-Band Reflectarray System Design

3.1. Aperture Efficiency Analysis

An aperture efficiency analysis is carried out to determine the physical dimensions of the reflectarray. The reflectarray antenna configuration is given in Figure 4. The reflectarray is illuminated with a horn antenna. During the measurements, OBHL180400 double-ridged horn antenna that operates in the 18–40 GHz frequency range will be used. Thus, characteristics of this antenna are used to observe the aperture efficiency. If the feed antenna is approximated with the cos^q function, $q = 11$ at 30 GHz. The far-field distance of the feed antenna is calculated as 154 mm at 20 GHz and 231 mm at 30 GHz. Since the feed antenna is meant to be positioned to the far-field region in both cases, the distance of the phase center in the z direction is chosen as $H = 250$ mm. In the reflectarray design, we aimed to direct the reflected beam towards $\theta_o = 20^\circ$ in the $\phi = 0^\circ$ plane. And the predefined feed antenna is placed to $\theta_f = -20^\circ$ in the $\phi = 0^\circ$ plane. By the aperture analysis [30], the physical structure of the reflectarray that would work with the highest efficiency is obtained for the given requirements. Aperture efficiency (η_a), illumination efficiency (η_i) and spillover efficiency (η_s) are given in Figure 5 as the function of reflectarray diameter. Aperture efficiency, which is calculated by the product of illumination and spillover efficiencies, shows highest performance at $D = 250$ mm and $D = 280$ mm at 20 and 30 GHz, respectively. By considering the physical size of the available printed circuit boards in our laboratory, the diameter of the reflective surface for the prototype is chosen as $D = 198$ mm, which results in aperture efficiency of approximately $\eta_a = 0.69$ for both bands. The resulting reflective surface consists of 33 unit cells along its diameter.

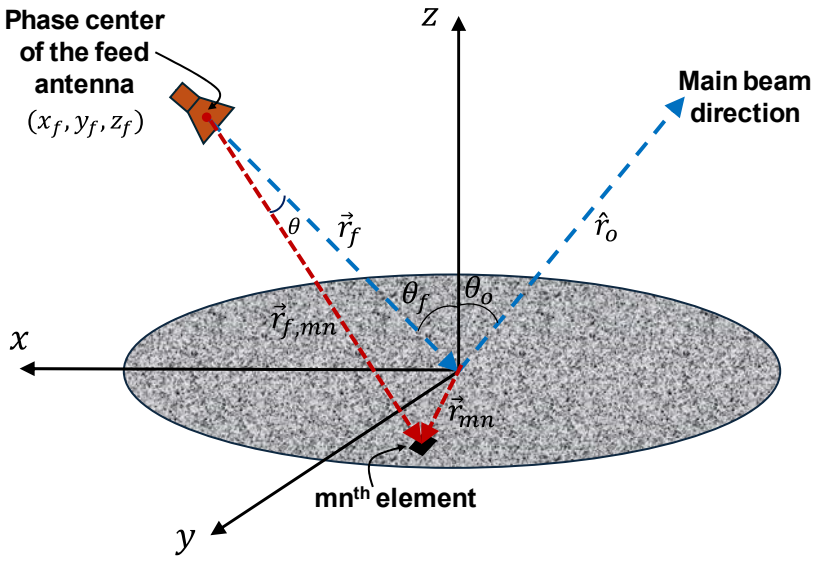

Figure 4. Reflectarray antenna configuration.

3.2. Reflective Surface Design at 20/30 GHz

To direct the beam reflected from the reflectarray surface towards predefined direction, the phase angle of each unit cell on the reflectarray should be calculated. Equation (2) is used to calculate the distance $r_{f,mn}$ of each unit cell from the phase center of the feed antenna, while Equation (3) is used to calculate the corresponding phases (ψ_{mn}) required to direct the beam.

$$r_{f,mn} = \sqrt{\left(x_{mn} - r_{f_x}\right)^2 + \left(y_{mn} - r_{f_y}\right)^2 + \left(z_{mn} - r_{f_z}\right)^2} \quad (2)$$

$$\psi_{mn} = k_0\left(r_{f,mn} - \vec{r}_{mn}.\hat{r}_0\right) + \psi_o \quad (3)$$

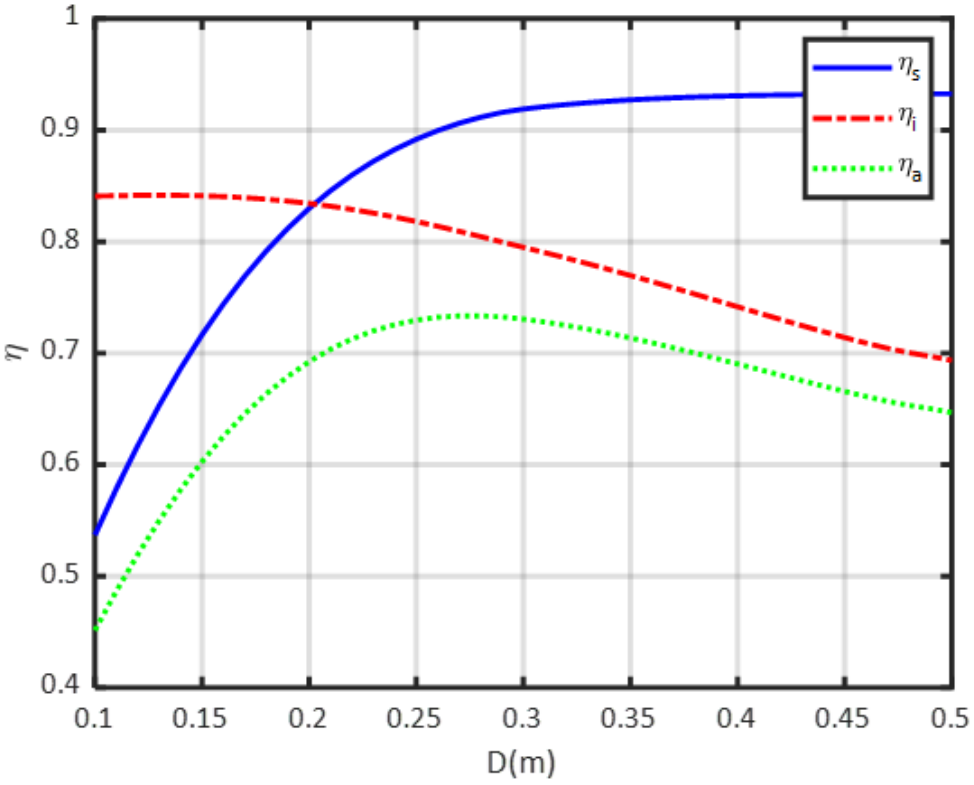

(**a**)

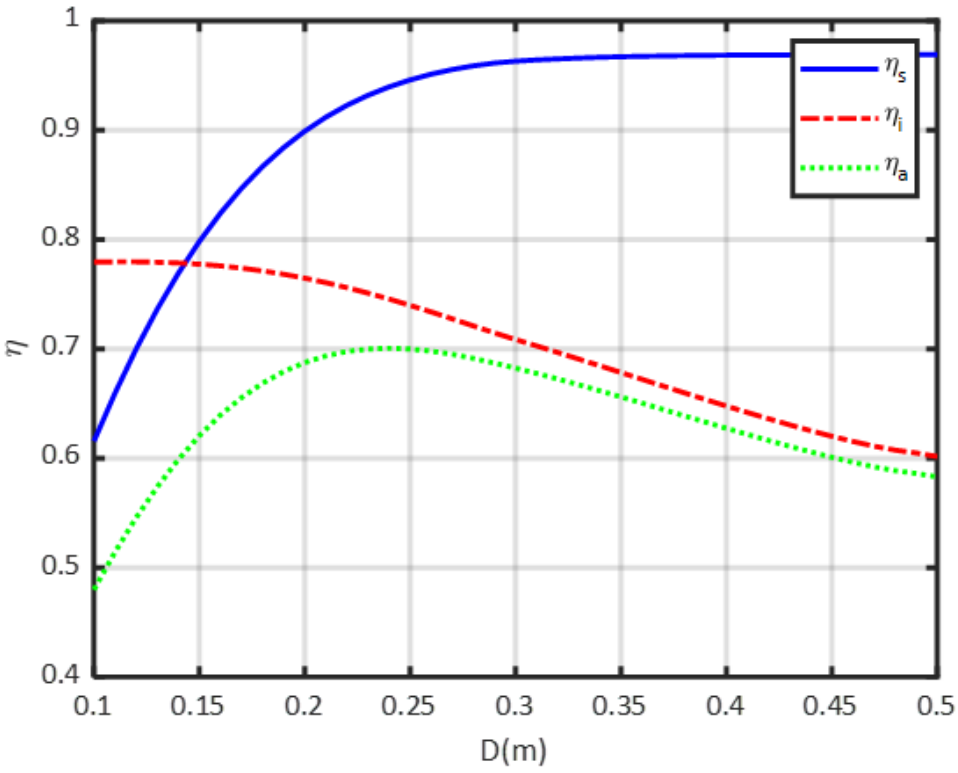

(**b**)

Figure 5. Aperture efficiency at (**a**) 20 GHz and (**b**) 30 GHz.

$\vec{r}_{mn}$ is the position vector of the mnth element, k_0 is the wave number, ψ_o is the phase constant, and $\hat{r}_0$ is the main beam direction [5]. r_{f_x}, r_{f_y}, and r_{f_z} in Equation (2) are the (x, y, z) components of the feed position. The phase distribution on the reflectarray surface is matched with the unit cell size given in Figure 2. For each of the unit cell on the reflective surface, the element dimension should give the phase value obtained using Equation (3). The phase patterns of the reflectarray consisting of 33×33 unit cells are obtained at 20 and 30 GHz for $D = 198$ mm, $\theta_o = 20°$, and $\theta_f = -20°$ in the $\phi = 0°$ plane, as given in Figure 6. The vertical distance between the reflective surface and the phase center of the feed antenna is set to $H = 250$ mm for 30 GHz. Since the phase center position of an antenna varies as the function of frequency, the phase center of the feed horn antenna at 20 and 30 GHz would be different from each other. By considering the phase center position at 20 GHz and reflective surface position compared to the reflective surface of 30 GHz, 5.18 mm is added to H to determine the corresponding phases of the unit cells for 20 GHz reflectarray.

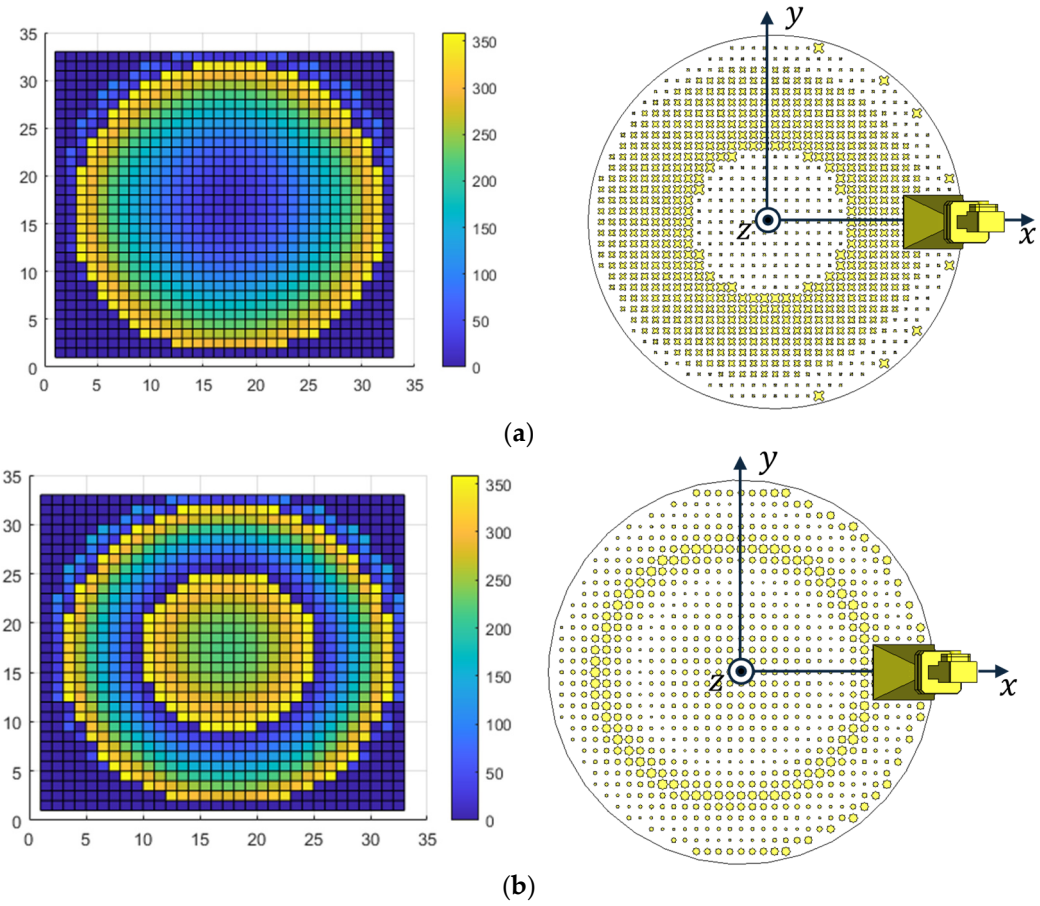

Figure 6. Phase distribution and corresponding reflectarray surface at (**a**) 20 GHz and (**b**) 30 GHz.

3.3. Results

The reflectarray antenna is required to steer the beam towards $\theta_o = 20°$ at both 20 GHz and 30 GHz frequencies. The feed antenna is located to (91 mm, 0 mm, 250 mm) of the coordinate system. Firstly, each of the reflectarrays are simulated separately. The performance levels of the single layer reflectarrays are also analyzed analytically using array theory. Figure 7 shows the simulated and calculated normalized radiation pattern of the reflectarrays in $\phi = 0°$ plane. It should be noted that, in this figure, a 30 GHz reflectarray is simulated with a whole copper ground plane (without FSS and 20 GHz reflectarray). Similarly, a 20 GHz reflectarray is simulated without FSS and 30 GHz reflectarray layers. The main beam is oriented towards $\theta_o = 20°$ with both reflectarrays. The directivities of the single layer reflectarrays are obtained as 22.5 dB and 24.8 dB at 20 and 30 GHz, respectively.

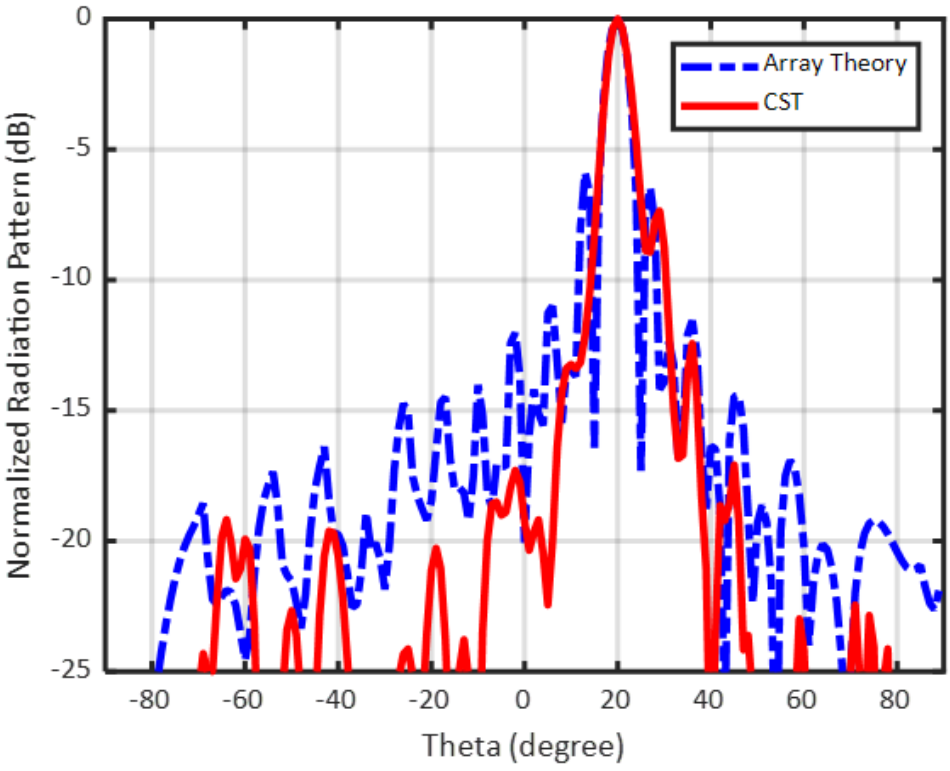

(**a**)

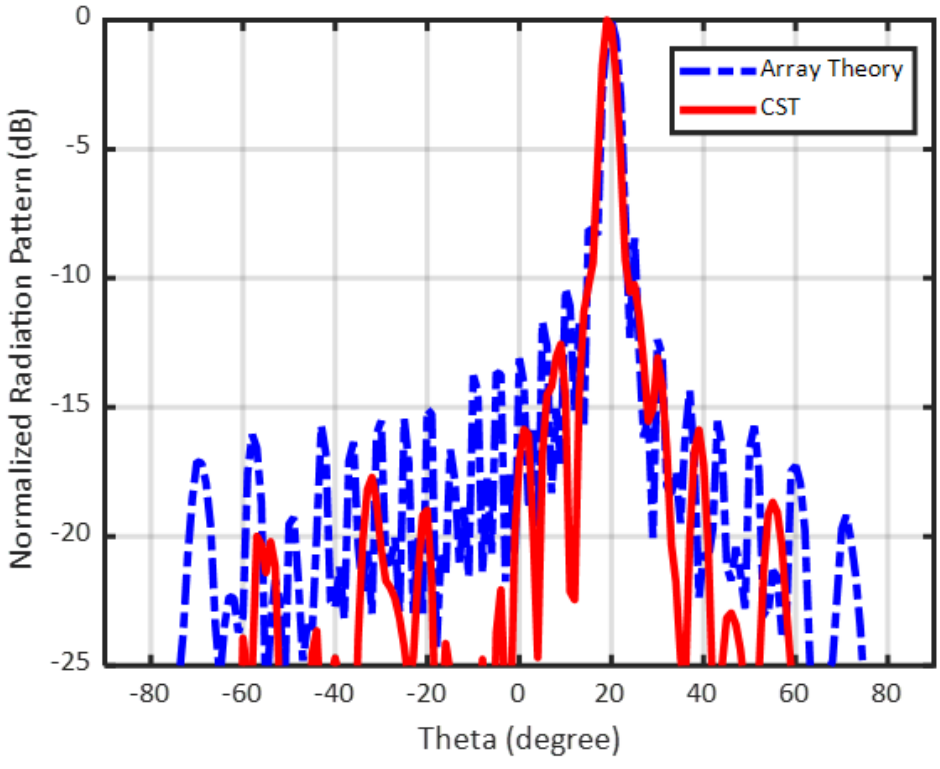

(**b**)

Figure 7. Normalized radiation patterns of the reflectarrays in $\phi = 0^{o}$ plane: (**a**) 20 GHz reflectarray; (**b**) 30 GHz reflectarray.

The multilayer reflectarray system consisting of the 30 GHz reflectarray at the top, 20 GHz reflectarray at the bottom, and FSS in between is given in Figure 8. As exhibited in this figure, the FSS structure is sandwiched between the two reflective surfaces. Simulated three-dimensional directivity patterns of the reflectarray at 20 and 30 GHz are given in Figure 9. The maximum directivity of the reflectarray antenna system is obtained as 20.9 dB at 20 GHz, 21.8 dB at 20.9 GHz, and 24.9 dB at 30 GHz. The figure clearly shows that the beam is oriented to $\theta_o = 20^\circ$ at both target frequencies. Normalized radiation patterns of the dual-band FSS-backed reflectarray system are given in Figure 10 in $\phi = 0^\circ$ plane. Higher sidelobes are observed at 20 GHz. However, they are still below the -10 dB level.

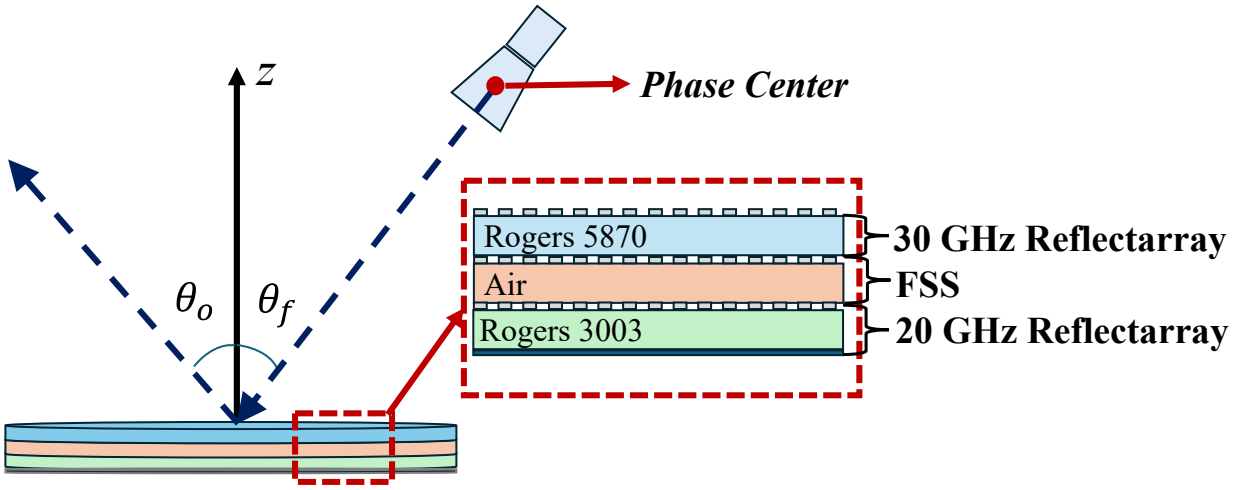

Figure 8. Dual-band FSS-backed reflectarray system.

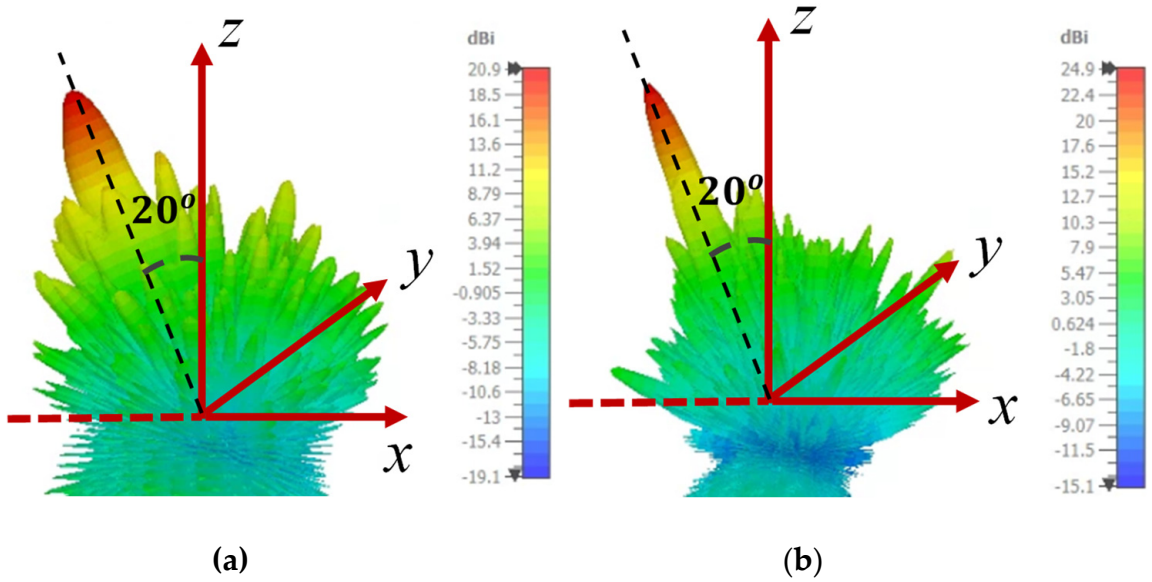

(a) **(b)**

Figure 9. Directivity patterns of the FSS-backed reflectarray system at (**a**) 20 GHz and (**b**) 30 GHz.

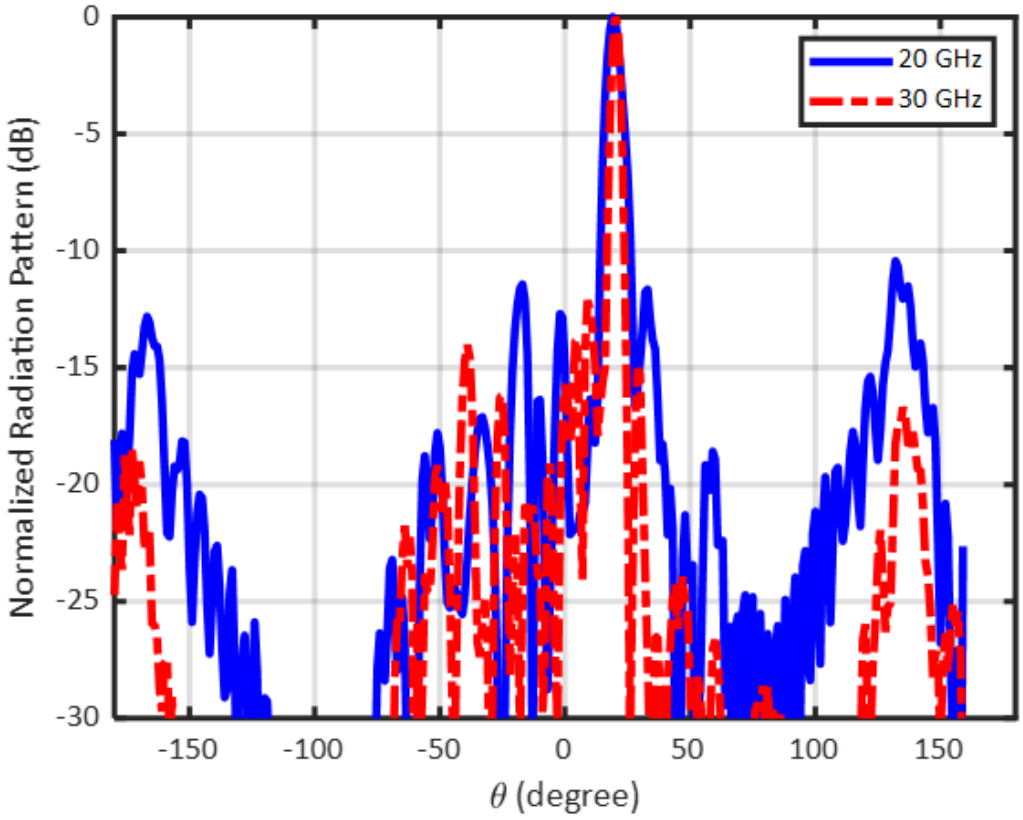

Figure 10. Normalized radiation patterns of the dual-band FSS-backed reflectarray system in $\phi = 0^\circ$ plane.

4. Experimental Verification

4.1. Fabrication of the Dual-Band Reflectarray

The reflective surfaces with 33-unit cells along their diameter are printed on a 200 mm × 200 mm Roger 5870 and Rogers 3003 printed circuit boards by chemical etching technique. Top and bottom views of the boards are given in Figure 11. All conductors are copper with a 35 µm thickness. Screwing holes with 5 mm diameter have been added to the corners of each reflective surface. A holder is fabricated by additive manufacturing technique using polylactic acid (PLA) material. By using the fabricated holder, the reflectarrays and the feed antenna are fixed to their positions as given in Figure 12. A 1 mm air gap between the reflectarrays is preserved by utilizing foam, which has a relative permittivity very close to air. The 18–40 GHz broadband double-ridged horn feed antenna is attached to the holder at $\theta = 20^\circ$ in the $\phi = 0^\circ$ plane. Reflectarrays and the foam is attached to the planar surface of the holder by four 5 mm screws.

4.2. Measurement Results

The dual-band reflectarray is measured with a 40 GHz Anritsu Vector Network Analyzer. The scattering parameters and radiation pattern of the reflectarray system are measured. The measurement of the radiation pattern is carried out in $\phi = 0^\circ$ plane within $0^\circ \leq \theta \leq 90^\circ$ angular range. An identical double-ridged horn antenna is used as the reference antenna in the measurements. The reflectarray antenna in the measurement setup is shown in Figure 13.

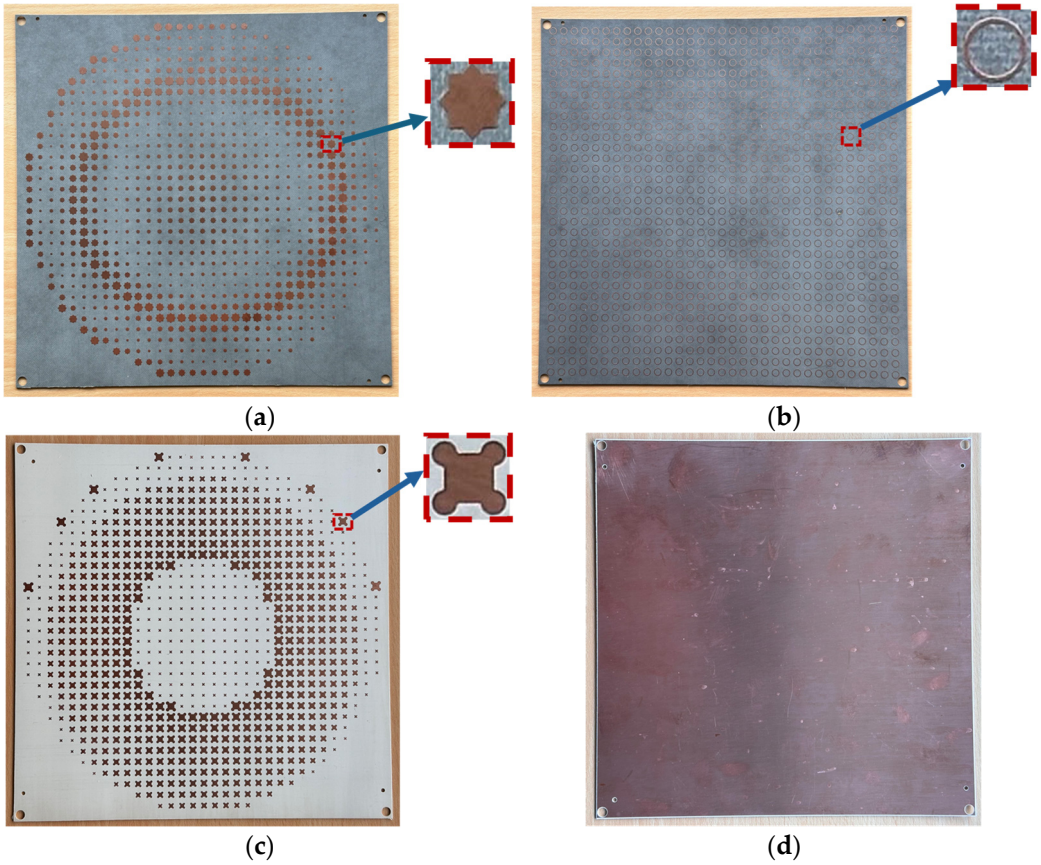

Figure 11. Fabricated printed circuit boards of the reflectarray: (**a**) top side of 30 GHz reflectarray; (**b**) bottom side of 30 GHz reflectarray (FSS surface); (**c**) top side of 20 GHz reflectarray; (**d**) bottom side of 20 GHz reflectarray.

The measured reflection coefficient of the dual-band reflectarray is given in Figure 14. The S_{11} variation in the reflectarray as the function of frequency shows that impedance matching is observed for the frequencies above 18 GHz. This result is expected due to the cutoff frequency of the horn antenna with a WR42 waveguide—2.92 mm connector adapter. When the uplink and downlink frequencies of the Ka-band satellites are considered, we can conclude that the system work properly in terms of impedance matching. Measures normalized radiation patterns of the dual-band reflectarray in $\phi = 0^\circ$ plane are given in Figure 15. Co- and cross-polarized patterns are shown at 20 and 30 GHz within $0^\circ \leq \theta \leq 90^\circ$ angular range. Compatible with the simulation and array theory results, beam radiation towards $\theta = 20^\circ$ is observed in both simulations. The crosspol level is about -35 dB at both 20 and 30 GHz patterns. The maximum gain of the reflectarray is measured as 21.13 dBi and 26.94 dBi at 20 and 30 GHz, respectively. A 3 dB beamwidth of the co-polarized pattern at 20 GHz is observed as 5.3°, where it reduces to 3.8° at 30 GHz. And 3 dB beamwidths of the measured patterns are almost identical to the simulated patterns. The aperture efficiency of 55% and 51% are achieved at 30 and 20 GHz, respectively. The reduction in the efficiency at the upper and lower bands are attributed to the narrowed reflection phase range due to the FSS structure. Measured gain variation in the dual-band reflectarray at Ka-Band satellite downlink and uplink frequencies are given in Figure 16. The blue and pink shaded areas show the downlink and uplink frequency ranges, respectively. The results show that the proposed dual-band FSS-backed reflectarray is suitable for high-speed Ka-band satellites.

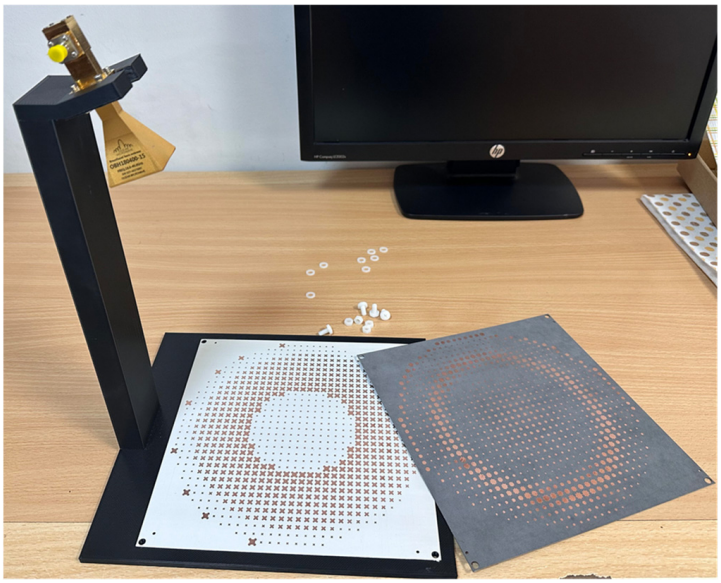

(**a**)

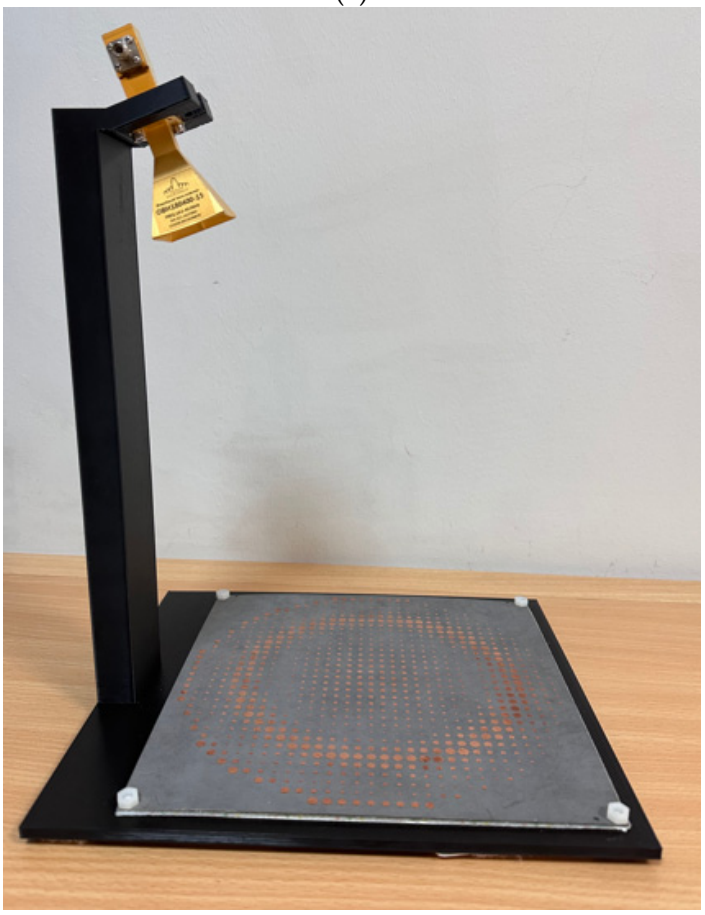

(**b**)

Figure 12. Prototype of the fabricated reflectarray system and the holder: (**a**) before assembling; (**b**) side view of the assembled prototype.

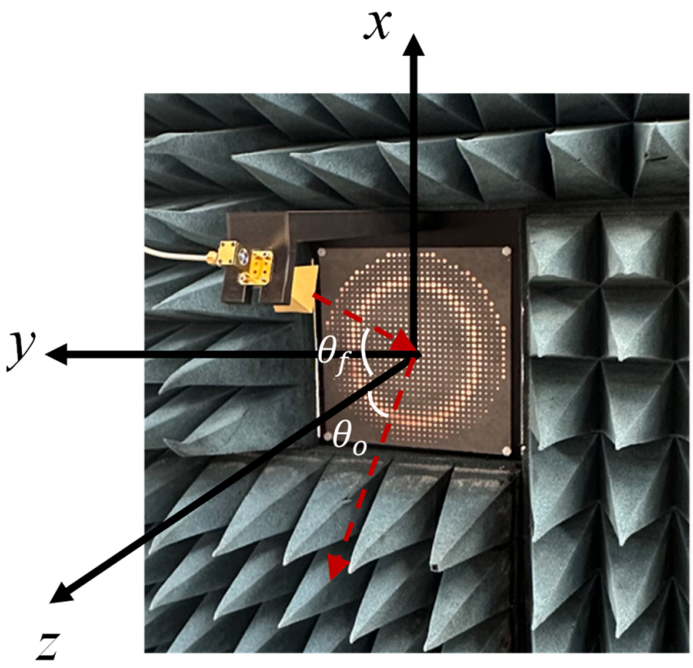

Figure 13. Measurement setup of the reflectarray system.

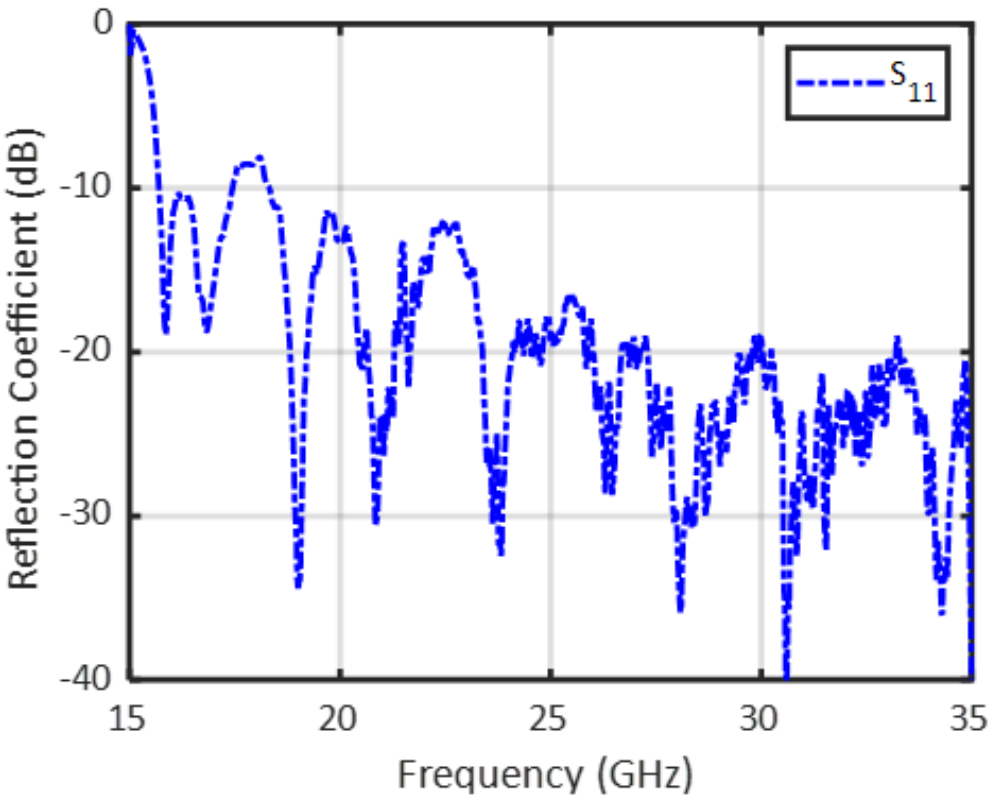

Figure 14. Measured reflection coefficient variation in the reflectarray.

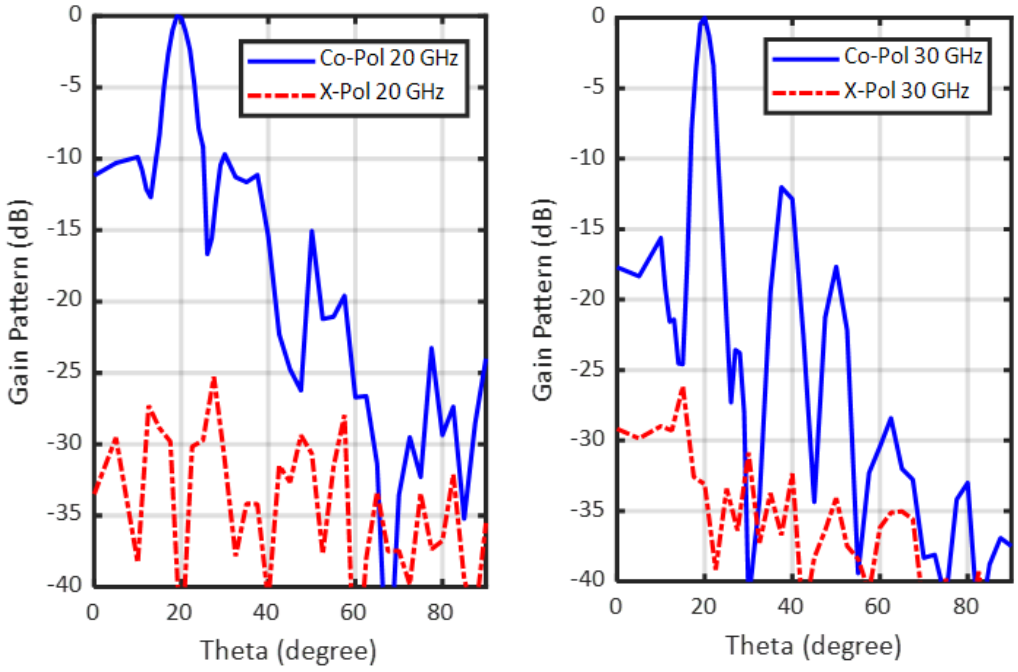

(**a**) (**b**)

Figure 15. Measured normalized gain patterns of the dual-band reflectarray: (**a**) 20 GHz; (**b**) 30 GHz.

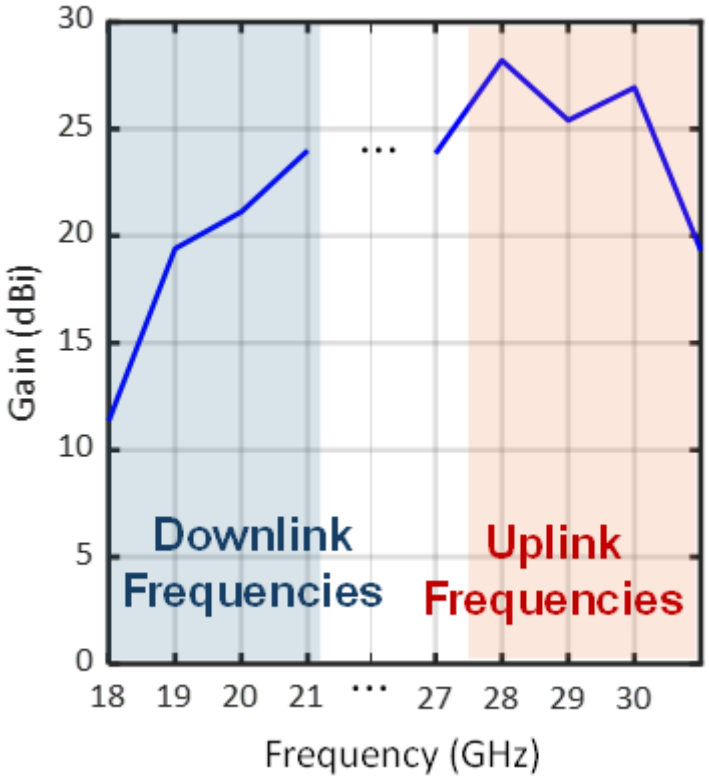

Figure 16. Measured gain variation in the dual-band reflectarray at Ka-Band satellite downlink and uplink frequencies.

5. Conclusions

In this work, a dual-band dual linear polarized reflectarray system is proposed for high-speed satellites operating at Ka-band Tx-Rx frequencies (20/30 GHz). An FSS consisting of

microstrip ring elements is used as the planar filter that acts as a ground layer at 30 GHz and permits the transmission of the wave at 20 GHz. Compared to dual-band counterparts that are designed on a single reflective surface, improved gain and aperture efficiency is obtained by suppressing the mutual coupling generated due to the elements of the two reflectarrays. Dual-polarized unit cells are used for the reflectarrays.

A dual-band reflectarray system, where the feed antenna is located at $\theta = -20^\circ$ in the $\phi = 0^\circ$ plane and the reflected wave is directed to $\theta = 20^\circ$ in the $\phi = 0^\circ$ plane is demonstrated. Its performance is analyzed by full wave analysis and the analytical method. The maximum directivity of 20.9 dB at 20 GHz, 21.8 dB at 20.9 GHz, and 24.9 dB at 30 GHz is obtained by the reflectarray antenna system. A prototype is fabricated, and the performance of the reflectarray designed for transmit/receive operation is experimentally verified. The results show that the proposed dual-band reflectarray system can be used in high-speed Ka-band satellites.

Author Contributions: Conceptualization, A.H.G. and N.T.T.; methodology, A.H.G. and N.T.T.; software, A.H.G.; validation, A.H.G., N.T.T. and A.A.; formal analysis, A.H.G.; investigation, A.H.G. and N.T.T.; resources, A.H.G. and N.T.T.; data curation, A.H.G.; writing—original draft preparation, A.H.G.; writing—review and editing, N.T.T. and A.A.; visualization, A.H.G. and N.T.T.; supervision, N.T.T.; project administration, N.T.T.; funding acquisition, N.T.T. All authors have read and agreed to the published version of the manuscript.

Funding: This work was supported by The Research Fund of Yildiz Technical University (Project Number: FBA-2021-4493).

Institutional Review Board Statement: Not applicable.

Informed Consent Statement: Not applicable.

Data Availability Statement: Data sharing is not applicable.

Conflicts of Interest: The authors declare no conflict of interest.

References

1. Corici, M.; Liolis, K.; Politis, C.; Geurtz, A.; Cahill, J.; Bunyan, S.; Schlichter, T.; Völk, F.; Kapovits, A. Satellite is 5G: SATis5. Whitepaper, European Space Agency: Paris, France, November 2020.
2. Rahmat-Samii, Y.; Densmore, A.C. Technology Trends and Challenges of Antennas for Satellite Communication Systems. *IEEE Trans. Antennas Propagat.* **2015**, *63*, 1191–1204. [CrossRef]
3. Singarajah, K. Overview of Ka-band Satellite System Developments & Key Regulatory Issues. In Proceedings of the ITU Conference on Prospects for Use of The Ka-Band by Satellite Communication Systems, Almaty, Kazakhstan, 5–7 September 2012.
4. Yao, Y.; Lin, X.Q.; Qin, T.; Su, Y.; Yang, X. Shared-Aperture Ka-Band Reflectarray and X-Band Phased Array for Broadband Inter-Satellite Communication. *IEEE Trans. Antennas Propagat.* **2022**, *70*, 11199–11204. [CrossRef]
5. Nayeri, P.; Yang, F.; Elsherbeni, A.Z. *Reflectarray Antennas: Theory, Designs, and Applications*; John Wiley & Sons: Hoboken, NJ, USA, 2018; p. 432.
6. Huang, J.; Encinar, J.A. *Reflectarray Antennas*; IEEE Press: Piscataway, NJ, USA, 2008.
7. Pozar, D.M. Bandwidth of reflectarrays. *Electron. Lett.* **2003**, *39*, 1490–1491. [CrossRef]
8. Mayumi, K.; Deguchi, H.; Tsuji, M. Wideband single-layer microstrip reflectarray based on multiple-resonance behavior. In Proceedings of the 2008 IEEE Antennas and Propagation Society International Symposium, San Diego, CA, USA, 5–11 July 2008; pp. 1–4. [CrossRef]
9. Yu, A.; Yang, F.; Elsherbeni, A.; Huang, J. Design and measurement of a circularly polarized Ka-band reflectarray antenna. In Proceedings of the 2009 3rd European Conference on Antennas and Propagation, Berlin, Germany, 23–27 March 2009; pp. 2769–2773.
10. Mohammadirad, M.M.; Komjani, N.; Sebak, A.R.; Chaharmir, M.R. A Broadband Reflectarray Antenna using the Triangular Array Configuration. *ACES J.* **2022**, *26*, 640–650.
11. Yusop, S.H.; Misran, N.; Islam, M.T.; Ismail, M.Y. Design of High-Performance Dual Frequency Concentric Split Ring Square Element for Broadband Reflectarray Antenna. *ACES J.* **2012**, *27*, 334–339.
12. Wu, D.I.; Hall, R.C.; Huang, J. Dual-frequency microstrip reflectarray. In Proceedings of the IEEE Antennas and Propagation Society International Symposium 1995 Digest, Newport Beach, CA, USA, 18–23 June 1995; pp. 2128–2131. [CrossRef]
13. Encinar, J.A. Design of a dual frequency reflectarray using microstrip stacked patches of variable size. *Electron. Lett.* **1996**, *32*, 1049. [CrossRef]

14. Chaharmir, M.R.; Shaker, J.; Gagnon, N.; Lee, D. Design of Broadband, Single Layer Dual-Band Large Reflectarray Using Multi Open Loop Elements. *IEEE Trans. Antennas Propagat.* **2010**, *58*, 2875–2883. [CrossRef]
15. Yu, A.; Yang, F.; Elsherbeni, A.Z.; Huang, J.; Kim, Y. An Offset-Fed X-Band Reflectarray Antenna Using a Modified Element Rotation Technique. *IEEE Trans. Antennas Propagat.* **2012**, *60*, 1619–1624. [CrossRef]
16. Han, C.; Rodenbeck, C.; Huang, J.; Chang, K. A C/Ka Dual Frequency Dual Layer Circularly Polarized Reflectarray Antenna with Microstrip Ring Elements. *IEEE Trans. Antennas Propagat.* **2004**, *52*, 2871–2876. [CrossRef]
17. Smith, T.; Gothelf, U.; Kim, O.S.; Breinbjerg, O. An FSS-Backed 20/30 GHz Circularly Polarized Reflectarray for a Shared Aperture L- and Ka-Band Satellite Communication Antenna. *IEEE Trans. Antennas Propagat.* **2014**, *62*, 661–668. [CrossRef]
18. Hasani, H.; Peixeiro, C.; Skrivervik, A.K.; Perruisseau-Carrier, J. Single-Layer Quad-Band Printed Reflectarray Antenna with Dual Linear Polarization. *IEEE Trans. Antennas Propagat.* **2015**, *63*, 5522–5528. [CrossRef]
19. Deng, R.; Yang, F.; Xu, S.; Li, M. An FSS-Backed 20/30-GHz Dual-Band Circularly Polarized Reflectarray with Suppressed Mutual Coupling and Enhanced Performance. *IEEE Trans. Antennas Propagat.* **2017**, *65*, 926–931. [CrossRef]
20. Zhu, X.-C.; Zhang, P.-P.; Zhang, Y.-X.; Ge, J.-X.; Gao, Z.-H. A High-Gain Filtering Antenna Based on Folded Reflectarray Antenna and Polarization-Sensitive Frequency Selective Surface. *Antennas Wirel. Propag. Lett.* **2020**, *19*, 1462–1465. [CrossRef]
21. Zhong, X.; Xu, H.-X.; Chen, L.; Li, W.; Wang, H.; Shi, X. An FSS-Backed Broadband Phase-Shifting Surface Array with Multimode Operation. *IEEE Trans. Antennas Propagat.* **2019**, *67*, 5974–5981. [CrossRef]
22. Xu, P.; Li, L.; Li, R.; Liu, H. Dual-Circularly Polarized Spin-Decoupled Reflectarray With FSS-Back for Independent Operating at Ku/Ka-Bands. *IEEE Trans. Antennas Propagat.* **2021**, *69*, 7041–7046. [CrossRef]
23. Li, J.; Mao, L.; Zhang, T. FSS Sandwiched Dual-Frequency Reflectarray for Mobile Communication Applications. *Electronics* **2023**, *12*, 897. [CrossRef]
24. Tahseen, M.M.; Kishk, A.A. Flexible and Portable Textile-Reflectarray Backed by Frequency Selective Surface. *Antennas Wirel. Propag. Lett.* **2018**, *17*, 46–49. [CrossRef]
25. Li, L.; Chen, Q.; Yuan, Q.; Sawaya, K.; Maruyama, T.; Furuno, T.; Uebayashi, S. Frequency Selective Reflectarray Using Crossed-Dipole Elements with Square Loops for Wireless Communication Applications. *IEEE Trans. Antennas Propagat.* **2011**, *59*, 89–99. [CrossRef]
26. Gülseren, A.H.; Alparslan, A.; Tokan, N.T. Dual Band Linear Polarized Reflectarray System with FSS Backing. In Proceedings of the 14th International Conference on Electrical and Electronics Engineering (ELECO), Bursa, Turkiye, 30 November–2 December 2023; pp. 1–5. [CrossRef]
27. *CST Microwave Studio*; ver. 20022; Computer Simulation Technology: Framingham, MA, USA, 2008.
28. de Rioja del Nido, E.M.M. New Advances on Multi-Frequency and Multi-Beam Reflectarrays with Application to Satellite Antennas in Ka-band. PhD Thesis, Universidad Politécnica de Madrid, Madrid, Spain, 2018. [CrossRef]
29. Shaker, J.; Chaharmir, M.R.; Ethier, J. *Reflectarray antennas: Analysis, Design, Fabrication and Measurement*; The Artech House Antennas and Propagation Series; Artech House: Boston, UK, 2014.
30. Yu, A.; Yang, F.; Elsherbeni, A.Z.; Huang, J.; Rahmat-Samii, Y. Aperture efficiency analysis of reflectarray antennas. *Microw. Opt. Technol. Lett.* **2010**, *52*, 364–372. [CrossRef]